2002

Stability-induced modification of sea surface winds over Gulf Stream rings

Kyung-Ae Park
University of Rhode Island

Peter C. Cornillon
University of Rhode Island, pcornillon@uri.edu

Citation/Publisher Attribution

Park, K., & Cornillon, P. C. Stability-induced modification of sea surface winds over Gulf Stream rings, *Geophys. Res. Lett.*, 29(24), 2211, doi: 10.1029/2001GL014236, 2002.
Available at: https://doi.org/10.1029/2001GL014236

Stability-induced modification of sea surface winds over Gulf Stream rings

Kyung-Ae Park[1] and Peter C. Cornillon
University of Rhode Island, Narragansett, RI, USA

Received 25 October 2001; accepted 28 May 2002; published 27 December 2002.

[1] Satellite-borne scatterometer and infrared data collected over Gulf Stream warm and cold core rings are used to study the effect of the sea-air temperature difference on the wind speed over rings. The observed acceleration of the wind over warm core rings and deceleration over cold core rings is found to be consistent with that predicted by the planetary boundary layer model of *Brown and Foster* [1994]. In addition it is shown that the distance over which the winds respond to an ocean surface temperature step is short ($\leq$25km) while the distance over which the marine boundary layer responds to a surface temperature step is long ($\geq$175km). *INDEX TERMS:* 4504 Oceanography: Physical: Air/sea interactions (0312); 3339 Meteorology and Atmospheric Dynamics: Ocean/atmosphere interactions (0312, 4504); 3307 Meteorology and Atmospheric Dynamics: Boundary layer processes; 4275 Oceanography: General: Remote sensing and electromagnetic processes (0689); 4520 Oceanography: Physical: Eddies and mesoscale processes. **Citation:** Park, K.-A., and P. C. Cornillon, Stability-induced modification of sea surface winds over Gulf Stream rings, *Geophys. Res. Lett.*, *29*(24), 2211, doi:10.1029/2001GL014236, 2002.

1. Introduction

[2] It has long been known that the stability of the marine boundary layer (MBL) depends on the sea-air temperature difference, $T_s - T_a$, and that the surface wind stress, $\vec{\tau}_s$, depends in turn on the stability of the marine boundary layer. These relationships have been examined in a number of studies [e.g., *Sweet et al.*, 1981, *Businger and Shaw*, 1984, *Liu*, 1984, *Wallace et al.*, 1989, *Friehe et al.*, 1991] involving open ocean observations. In the past several years, there has also been a number of studies addressing the relationship between satellite-derived surface winds and sea surface temperature (T_s) in the vicinity of ''tropical instability waves'' [*Xie et al.*, 1998, *Wentz et al.*, 2000, *Hashizume et al.*, 2001, *Chelton et al.*, 2001]. *Hashizume et al.* [2001] examine wind speed anomaly as a function of T_s anomaly while *Chelton et al.* [2001] obtain a relationship between the surface wind stress curl and divergence and the surface temperature gradient. Although the statistical relations derived are for T_s gradients or anomalies, the underlying assumption is that these quantities are representative of $T_s - T_a$ hence related to MBL stability.

[3] In this study we examine the relationship between satellite-derived 10 m equivalent neutral winds, $\vec{\mathbf{u}}_{10}^N$, and $T_s - T_a$. We conduct our study in the vicinity of Gulf Stream rings using the sea surface temperature difference between water in the ring and water that surrounds it as a proxy for $T_s - T_a$. Because Gulf Stream rings are closed structures it is possible to associate changes in $\vec{\mathbf{u}}_{10}^N$ with T_s steps, hence by assumption $T_s - T_a$ steps, normal to $\vec{\mathbf{u}}_{10}^N$. This obviates the need to rely on differential measures such as those used in *Chelton et al* [2001] to address a relationship that is inherently non-linear.

2. Data

[4] Data from two satellite-borne scatterometer missions have been used for this study: NSCAT [*Jet Propulsion Laboratory*, 1998] (September 1996 through June 1997), and QuikSCAT [*Jet Propulsion Laboratory*, 1999] (July 1999 through April 2000). The spatial resolution of both scatterometers is 25 km and the temporal sampling, although irregular depending on latitude and scatterometer design, is on the order of once per day at mid-latitude. The winds used in this study are the 10 m equivalent neutral winds, $\vec{\mathbf{u}}_{10}^N$, obtained from the Jet Propulsion Laboratory in Pasadena, California. These correspond to the winds that one would obtain from the friction velocity (the quantity effectively measured by the scatterometer) assuming an unstratified MBL. The uncertainty of the NSCAT data is on the order of 1.3 m/s and 20° for wind speeds ranging from 1 m/s to 18 m/s [*Freilich and Dunbar*, 1999]. The uncertainty of QuikSCAT is thought to be similar. We refer to $\vec{\mathbf{u}}_{10}^N$ as the scatterometer-derived winds in the following.

[5] T_s fields obtained from the University of Miami were used to locate Gulf Stream rings and to estimate the temperature inside and outside of the rings. The T_s fields were derived from infrared data collected by the Advanced Very High Resolution Radiometer (AVHRR) carried on NOAA polar orbiting satellites. There are typically two fields per day covering any mid-latitude location at approximately 1 km resolution. Processing of the AVHRR data is described in *Cornillon et al.* [1988].

[6] Each T_s field for the period during which the scatterometers were operating was examined for the existence of Gulf Stream rings. For those fields in which one or more rings were clearly visible, a representative outer boundary of each ring was manually digitized and an ellipse was fit to it in a least square sense [*Hooker and Olson*, 1984]. Different criteria were used to select the boundary digitized for warm core rings and cold core rings. Warm core rings are usually well defined in the T_s field as warm elliptical regions surrounded by a relatively large T_s gradient boundary. This is the boundary that was digitized. Cold core rings on the other hand are generally visible only shortly after they have formed or after a recent interaction with the Gulf Stream. In both cases the cold core is surrounded by a

[1]Now at Seoul National University, Seoul, Korea.

0094-8276/02/2001GL014236

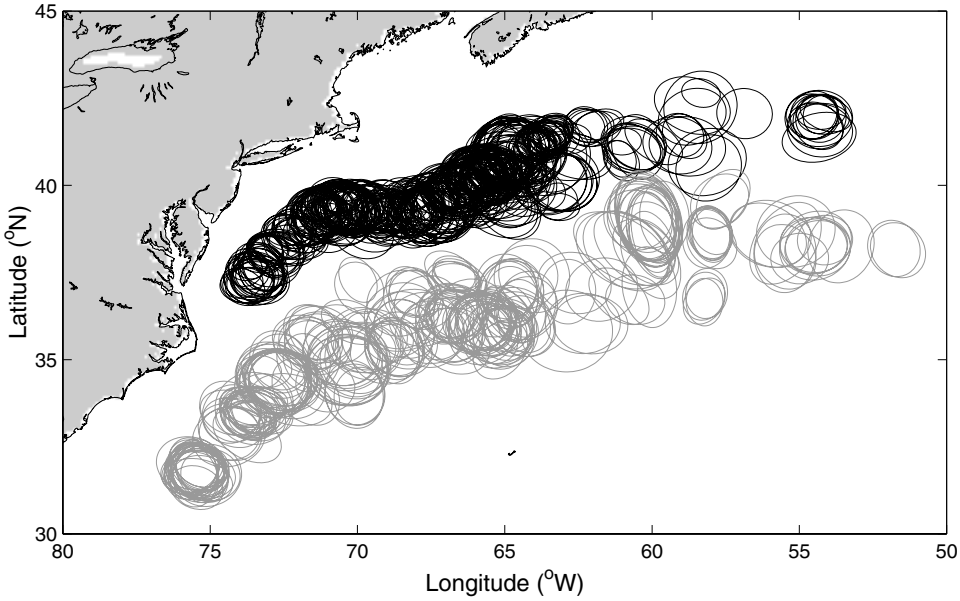

Figure 1. The location of Gulf Stream warm (black) and cold (gray) core ring observations used in this study. Each ellipse represents a fit to the outer contour of a ring observation manually digitized from an AVHRR-derived T_s field.

band of Gulf Stream water that is warmer than the Sargasso Sea water in which the ring is found. For the case of a recent interaction with the Gulf Stream, the majority of the observations used in this study, this band of warm water rarely encircles the ring, hence its edge does not define an isotach of the ring surface current. Digitizing the high gradient contour at the edge of this band does not yield a correct center for the ring. To address this problem, the center of this band was digitized. Although this approach yields a boundary that is less accurate than that for warm core rings the error is still small compared with the resolution of the scatterometer data used. The locations of all digitized rings are shown in Figure 1; 439 warm core ring observations were made in the Slope Water north of the stream and 260 cold core ring observations were made in the Sargasso Sea south of the stream.

[7] The T_s field for each ring observation was paired with one or more scatterometer passes that completely covered the ring and that occurred within 48 hours of the T_s observation. The meridional and zonal coordinates for both the T_s field and the corresponding wind field were scaled so that the digitized ring boundary formed a circle of radius one centered on the origin and both coordinate systems were then rotated so that the mean wind over the ring points in the positive y direction. The mean wind was determined for a region defined by a square of 11×11 scatterometer cells, 275×275 km, (13×13, 325×325 km, for rings that touched the boundaries of an 11×11 cell square) centered on the ring.

3. Results

[8] The upper eight panels of Figure 2 show the mean y-component (down-wind) of the scatterometer-derived wind in the normalized ring coordinate system for 3 m/s wind speed ranges from 3 to 15 m/s. For each of these ranges acceleration of the wind over warm core rings is well defined and there is a suggestion of deceleration over cold core rings. An acceleration/deceleration asymmetry of the down-wind speed in the cross-wind direction over the rings is also evident. This asymmetry, most clearly seen for cold core rings, results from the fact that the scatterometer measures the wind *relative* to the ocean surface [*Cornillon and Park*, 2001]. Specifically, the wind to the left (right) of a cold core ring center looking down-wind is moving against (toward) the ring current, hence the speed of the wind *relative* to the water surface is larger (smaller) to the left (right) of the ring center than the average. This is clearly seen in the lower two panels of Figure 2, which present the ratio of the y-component of the wind speed averaged over y inside the ring to the mean background y-component. The blue curves are for the idealized case of a uniform wind over the region and typical ring surface currents. The red curves are obtained from the data by averaging over all warm/cold core ring observations. In addition to the cross-wind asymmetry, the acceleration/deceleration is also clearly evident in these curves.

[9] The plots of Figure 2 also suggest that the spatial scale over which the wind adjusts to a change in the stability of the MBL is relatively small, order 25 km (or smaller); the acceleration seen clearly in the warm core ring case appears to take place within one grid element, generally less than 25 km, of the up-wind edge of the ring. This is consistent with the observations suggested by the plots in *Friehe et al.* [1991]. By contrast, the spatial scale over which the MBL returns to neutral stability following a step change in T_s is large compared with the typical ring diameter, $\approx$150 to 175 km. In all cases there is little change either in the acceleration/deceleration of the wind from the point at which the wind initially crosses the ring boundary to the opposite side of the ring or in the magnitude of the y-component of the wind down-wind of the ring compared with that up-wind of the ring.

[10] Figure 3 is a plot of $U_{10}^{N}(\text{in})/U_{10}^{N}(\text{out})$ versus $T_s(\text{in})-T_s(\text{out})$ for U_{10}^{N} (the component of $\vec{\mathbf{u}}_{10}^{N}$ in the direction of the vector averaged $\vec{\mathbf{u}}_{10}^{N}$ over the relevant

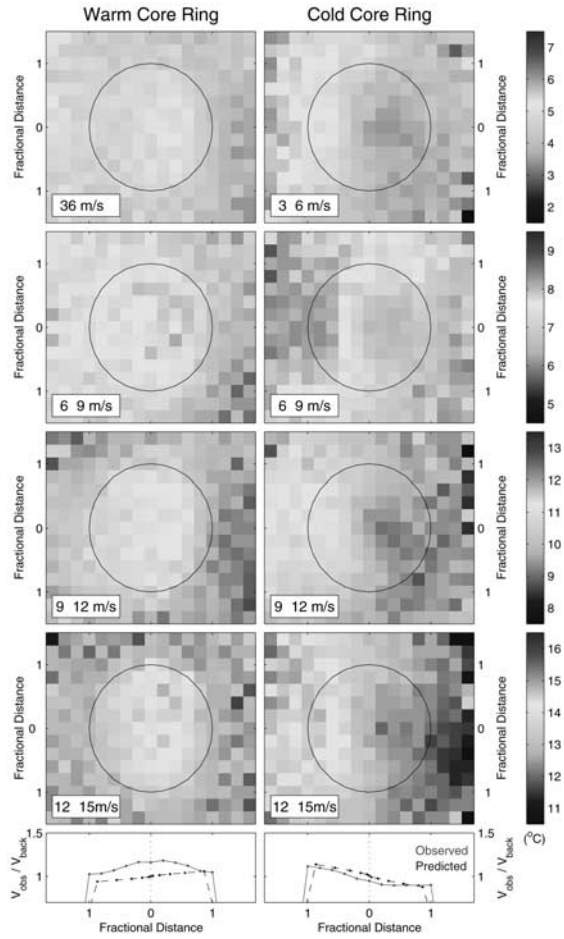

Figure 2. The downwind component of the scatterometer winds over Gulf Stream warm and cold core rings averaged and binned by mean background wind speed. Prior to averaging each scatterometer pass was rotated so that the mean wind points upward, the origin was relocated to the center of the best fit ellipse to the ring boundary and distances were normalized by the distance from the center to the best fit ellipse.

region) between 3 and 15 m/s in 3 m/s bins. "Out" refers to a vector average of U_{10}^N over the region outside of the ellipse defining the boundary of the ring but within a 275 × 275 km box centered on the ring. For warm core rings "in" refers to an average of the winds over the region with normalized radii less than 1.0 and for cold core rings a smaller inner radius of 0.5 was chosen to avoid contamination of the "interior" of the ring with the warm band of Gulf Stream water discussed above.

[11] Also plotted in Figure 3 are curves of $U_{10}^N(T_s - T_a)/U_{10}^N$ versus $T_s - T_a$ obtained from the University of Washington (UW) planetary boundary layer (PBL) model [*Brown and Liu*, 1982; *Brown and Foster*, 1994]. All model runs were performed for an atmospheric humidity of 78.7% and T_s of 19.52°C, climatological values based on the period 1989–1994 for the Gulf Stream region. The only parameters varied from simulation-to-simulation were the geostrophic forcing and $T_s - T_a$ although they were not allowed to vary during a simulation. For each point on the curves the same geostrophic forcing was used for both $U_{10}^N(T_s - T_a)$ and U_{10}^N. $U_{10}^N(T_s - T_a)$ was obtained by first calculating the magnitude of the friction velocity, u_*, associated with the given forcing and $T_s - T_a$ and then determining the magnitude of the equivalent neutral wind corresponding to u_* using the standard log relationship $U_{10}^N(T_s - T_a) = (u_*/k)\log(10/z_0 + \psi)$ with the stratification term, ψ, set to zero. k, the von Kármán constant is 0.4. U_{10}^N is the equivalent neutral winds for a neutrally stratified MBL. The PBL model is based on similarity theory which is valid only in a constant flux layer under quasi-stationary and horizontally homogeneous conditions. Despite this constraint and the fact that the model runs are for fixed meteorological and oceanographic conditions the shapes and magnitudes of the observed and modeled curves are quite similar.

[12] Part of the discrepancy between model results and scatterometer observations may result from the assumption that the MBL is neutrally stratified "outside" of the ring. Under such conditions T_s(out), the satellite-derived ocean surface temperature outside of the ring, approximates T_a, the air temperature used in the model; $T_s(\text{in}) - T_s(\text{out}) \approx T_s - T_a$; $U_{10}^N(\text{out}) \approx U_{10}^N$ and $U_{10}^N(\text{in}) \approx U_{10}^N(T_s - T_a)$. However, this will only be true if the surface water temperature, T_s, remains unchanged for a long distance up-wind of

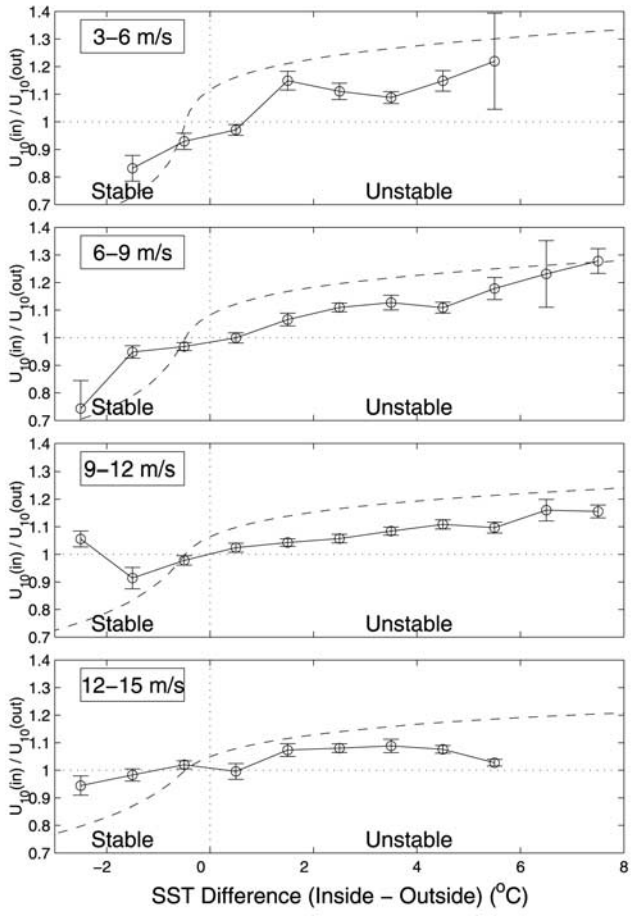

Figure 3. The ratio of the wind speed over a ring to that outside of the ring. Solid line with error bars observed U_{10}^N ratio versus T_s (in)−T_s (out); dashed curve modeled $U_{10}^N(T_s - T_a)/U_{10}^N$ versus $T_s - T_a$.

the ring, and this is rarely the case. In fact, for almost all cold core ring and approximately 3/4 of the warm core ring observations, there is a band of water outside of the ring with a temperature that lies between that of the ring and that beyond the band. For the remaining 1/4 of the warm core ring cases, T_s(out) was approximately equal to or slightly smaller than that several hundred kilometers upwind of the ring. Given the quick response of the wind to a change in surface temperature compared with the slow response of the MBL stability (described above), one would expect the observed wind speed ratios, U_{10}^N (in)/U_{10}^N (out), to be closer to 1.0 than the modeled ratios of the wind speed over the ring, U_{10}^N ($T_s - T_a$)/U_{10}^N. Basically, the wind speed outside the ring has adjusted to the change in surface temperature outside of the ring compared to the temperature upwind of this region but the MBL has not. As the wind blows over the T_s step at the ring boundary it adjusts again, but only to the incremental difference in temperature between the ring and the region beyond the band immediately outside of the ring. Because of the non-linearity of the wind speed ratio relative to $T_s - T_a$, the actual change in wind speed is smaller than it would have been had the MBL been neutrally stratified outside of the ring.

4. Conclusion

[13] In this paper we have documented the acceleration (deceleration) of scatterometer-derived equivalent neutral winds over warm (cold) core rings. We have also shown that the observed acceleration/deceleration is similar in magnitude as well as in its dependence on $T_s - T_a$ and wind speed with that predicted by the UW PBL model [*Brown and Foster*, 1994]. Specifically, the magnitude of the ratio,U_{10}^N (in)/U_{10}^N (out), for both warm and cold core rings decreases with increasing wind speed as does the modeled ratios, U_{10}^N ($T_s - T_a$)/U_{10}^N. Although there are other possible causes for the observed acceleration/deceleration, such as a change in surface friction due to changes in T_s, we believe that the similarity between our observations and the PBL model support attribution of the primary cause to changes in the stability of the MBL as it crosses a T_s step.

[14] We have also shown that the spatial scale over which the wind speed adjusts to a T_s step is small, less than 25 km, while that over which the MBL adjusts to the same T_s step is substantially larger, certainly greater than 175 km.

[15] Finally, we note that although these results have been presented in the context of changes in the vector winds as they flow over Gulf Stream rings, they in fact apply to changes in the winds as they flow over T_s steps in the ocean in general.

[16] **Acknowledgments.** This study was performed with support from the National Aeronautics and Space Administration (Grant NAS5-32965 via Oregon State University and Jet Propulsion Laboratory grant #957627) as part of the SeaWinds and NSCAT programs. Salary support for P. Cornillon was provided by the State of Rhode Island and Providence Plantations. The software used to process the AVHRR data was developed by R. Evans, O. Brown, J. Brown and A. Li of the U. Miami. Their continued support is greatly appreciated. Authors are grateful to David Long, Mike Freilich, and two unknown reviewers for their helpful discussions and comments related to this work. The model was obtained and run with the help of Robert Brown, Ralph Foster and Jérôme Pataux of the U. Washington.

References

Brown, R. A., and W. T. Liu, An operational large-scale planetary boundary layer model, *J. Applied Meteor.*, *21*, 261–269, 1982.

Brown, R. A., and R. C. Foster, On large-scale PBL modelling: The PBL models Atmos, *Ocean Syst.*, *2*, 163–184, 1994.

Businger, J. A., and W. J. Shaw, The response of the marine boundary layer to mesoscale variations in sea-surface temperature, *Dynamics Atmos. Oceans*, *8*, 267–280, 1984.

Chelton, D. B., S. K. Esbensen, M. G. Schlax, N. Thum, M. H. Freilich, F. J. Wentz, C. L. Gentemann, M. J. McPhaden, and P. S. Schopf, Observations of coupling between surface wind stress and sea surface temperature in the eastern Tropical Pacific, *J. Climate*, *14*, 1479–1498, 2001.

Cornillon, P., D. Evans, O. B. Brown, R. Evans, and J. Brown, Processing, compression and transmission of satellite IR data for near-real time use at sea, *J. Atmos. Tech.*, *5*, 320–327, 1988.

Cornillon, P., and K.-A. Park, Warm core ring velocities inferred from NSCAT, *Geophys. Res. Lett.*, *28*, 575–578, 2001.

Friehe, C. A., W. J. Shaw, D. P. Rogers, K. L. Davidson, W. G. Large, S. A. Stage, G. H. Crescenti, S. J. S. Khalsa, G. K. Greenhut, and F. Li, Air-sea fluxes and surface layer turbulence around a sea surface temperature front, *J. Geophys. Res.*, *96*, 8593–8609, 1991.

Freilich, M. H., and R. S. Dunbar, The accuracy of the NSCAT 1 vector winds: Comparisons with National Data Buoy Center buoys, *J. Geophys. Res.*, *104*, 11,231–11,246, 1999.

Hashizume, H., S.-P. Xie, W. T. Liu, and K. Takeuchi, Local and remote atmospheric response to tropical instability waves: A global view from space, *J. Geophys. Res*, *106*, 10,173–10,185, 2001.

Hooker, S. B., and D. B. Olson, Center of mass estimation in closed vortices: A verification in principle and practice, *J. Atmos. Tech.*, *1*, 247–255, 1984.

Jet Propulsion Laboratory, Science Data Product (NSCAT-2) User's Manual Ver.1.2, Overview and Geophysical Data Products, *JPL Manual*, Jet Proplusion Laboratory, Pasadena, California, 1998.

Jet Propulsion Laboratory, QuikSCAT Science Data Product User's Manual, *JPL Manual*, Jet Propulsion Laboratory, Pasadena, California, 1999.

Liu, W. T., The effects of the variations in sea surface temperature and atmospheric stability in the estimation of average wind speed by SEASAT-SASS, *J. Phys. Oceanogr.*, *14*, 392–402, 1984.

Sweet, W., R. Fett, J. Kerling, and P. LaViolette, Air-sea interaction effects in the lower troposphere across the north wall of the Gulf Stream, *Mon. Weather Rev.*, *109*, 1042–1052, 1981.

Wallace, J. M., T. P. Mitchell, and C. Deser, The influence of sea-surface temperature on surface wind in the eastern Equatorial Pacific: Seasonal and interannual variability, *J. Climate*, *2*, 1492–1499, 1989.

Wentz, F. J., C. Gentemann, D. Smith, and D. Chelton, Satellite measurements of sea surface temperature through clouds, *Science*, *288*, 847–850, 2000.

Xie, S.-P., M. Ishiwatari, H. Hashizume, and K. Takeuchi, Coupled ocean-atmosphere waves on the equatorial front, *Geophys. Res. Letters*, *25*, 3863–3866, 1998.

K.-A. Park, BK21 School of Earth and Environmental Sciences, Seoul National University, Seoul, 151-742, Korea. (pka@eddies.snu.ac.kr)

P. C. Cornillon, Graduate School of Oceanography, University of Rhode Island, Narragansett, RI 02882, USA. (pcornillon@gso.uri.edu)